COBEM 2021 26th International Congress of Mechanical Engineering
November 22-26, 2021, Virtual Congress, Brazil
ABCM Associação Brasileira de Engenharia e Ciências Mecânicas

COB-2021-1534
A HIERARCHICAL FINITE ELEMENT MODEL FOR MODAL ANALYSIS OF AIRCRAFT STRUCTURES

Eduardo W. da Cunha
Maurício V. Donadon
Antônio B. Guimarães Neto
Instituto Tecnológico de Aeronáutica, Av. Praça Marechal do ar, 50, 12228-900, São José dos Campos – SP.
ecunha@ita.br, donadon@ita.br, antonio@ita.br

Fernando J. O. Moreira
Embraer, Av. Brg. Faria Lima, 2170, 12227-901, São José dos Campos – SP.
fernando.moreira@embraer.com.br

Abstract. *This paper presents the use of hierarchical finite element method to perform modal analysis of flexible aircraft. This formulation is derived from the Hamilton's Principle and then applied to undamped free vibration analysis. It is simple to implement and favors a quick, easy and seamless possibility of change of the aircraft geometry and structural properties, such as the dihedral and sweep angles of the wing, which is an advantage in early phases of aircraft design. The results obtained demonstrate great accuracy when compared with the classical finite element formulation. This method has the potential to reduce computational cost in both convergence analysis and optimization process.*

Keywords: *hierarchical finite element, aircraft structures, modal analysis, free vibration analysis, finite element.*

1. INTRODUCTION

Finite Element Method (FEM) is traditionally used in static and structural dynamics analyses. It is based on approximating the solution by piecewise smooth shape functions, specially low degree (p) polynomials, on convex subdomains such as lines, triangles and rectangles (Babuška *et al.*, 1981). The conventional asymptotic convergence method is called h-version in which the degree p is kept bounded and the maximum diameter h of the elements approach zero by introducing new subdivisions. Once the new subdivisions are accomplished, a completely new solution and convergence observation are performed, leading the computer to discard the previously generated solution and repeat all the calculations to generate a new one (Zienkiewicz *et al.*, 1983), which is computationally expensive.

Another possibility of model refinement is, instead of the maximum diameter h of the elements approaching zero, to make the degree (p) of the approximating polynomials tend to infinity by introducing new polynomials of progressively ascending degree, while the subdomains are kept constant. This process is known as the p-version of the FEM (Babuška, 1988; De-Chao, 1986) and it is similar to a Taylor series expansion. As new terms are called, the previous terms remain unaltered and a single term is introduced at each step or convergence verification, the refinement ceasing when the accuracy of the solution is concluded to be sufficient. Therefore, the increase of n to $n + 1$ shape functions does not alter the former n: this is the definition of hierarchical (Zienkiewicz *et al.*, 1983; De-Chao, 1986). For that reason the p-version of FEM is also known as Hierarchical Finite Element Method (HFEM).

HFEM has the potential to enhance structural analysis performance in several ways, such as: previously storing precalculated matrices with a high number of hierarchical shape functions, speeding up and automatizing convergence analysis, improving optimization process and parameterizing input data (such as geometry and material properties). Therefore, applying HFEM in aircraft structures analysis or in flight dynamics analysis of flexible aircraft, for instance, in early phases of aircraft design, enables a higher fidelity modeling, which can be computationally cheaper than classical FEM. This paper presents an initial stage of HFEM implementation, with a modal analysis of aircraft structure – which is useful in the fields of mechanical vibrations and flight dynamics – and a comparison of results with classical FEM as well.

2. BARDELL'S SERIES OF EQUATIONS

A problem of concern regarding HFEM is the choice of the hierarchical series of equations, due to the difficulty of accurately calculating all the integrals of the stiffness and mass matrices of high order elements (De-Chao, 1986; Bardell, 1989). With that in mind, De-Chao (1986) suggested the use of Rodrigues' formulation of Jacobi orthogonal polynomials to develop a hierarchical series of equations. Bardell (1989) developed two series of equations, using Rodrigues' form of

Legendre polynomials and then applied in free vibration analysis of a plate (Bardell, 1991).

Recently, de Sena e Oliveira (2018) used Bardell's series in plate analysis in several different scenarios, performed convergence analysis and compared the results with the literature for each one of them, coming to the conclusion that the obtained results have excellent accuracy. Also, Bernardino (2019) compared the results of buckling analysis from several flat panels configurations using both Bardell's polynomials and the trigonometric hierarchical series from Beslin and Nicolas (1997), concluding that the polynomial series converges faster than the trigonometric. Therefore, it is possible to observe the robustness of Bardell's series in static as well as dynamic analysis.

As mentioned previously, Bardell (1989) developed two hierarchical series derived from the Rodrigues' form of Legendre orthogonal polynomials. They are:

$$g_r(\xi) = \sum_{n=0}^{r/2} \frac{(-1)^n (2r-2n-5)!!}{2^n n!(r-2n-1)!} \xi^{r-2n-1} \qquad (r>2) \tag{1}$$

$$f_r(\xi) = \sum_{n=0}^{r/2} \frac{(-1)^n (2r-2n-7)!!}{2^n n!(r-2n-1)!} \xi^{r-2n-1} \qquad (r>4) \tag{2}$$

where $r!! = r(r-2)...(2 \text{ or } 1)$, $0!! = (-1)!! = 1$, $r/2$ denotes its own integer part and $\xi = 2x/L - 1$ is the natural coordinate (Bardell, 1989). Those series are applicable to problems involving in-plane (tension and/or torsion) and out-of-plane (bending) motion, respectively. The first two linear in-plane functions and the first four cubic out-of-plane functions are identical to those used in classical FEM, which means they are not generated from Equations (1) and (2). These functions describe the boundary conditions, i. e. the elastic displacement (for both) and slope (only for the out-of-plane motion) at the boundaries of the problem's domain. All the higher order ($r > 2$) in-plane functions have zero displacement and non-zero slope at each end of the element. Similarly, all the higher order ($r > 4$) out-of-plane functions have both zero displacement and zero slope at the edges of the element. Therefore, all the higher order of both in-plane and out-of-plane functions represent the internal elastic displacement field of the element.

3. STRUCTURAL MODEL

3.1 Aircraft Model and Discretization

An example aircraft can be discretized in eight beam elements, as shown in Figure 1.

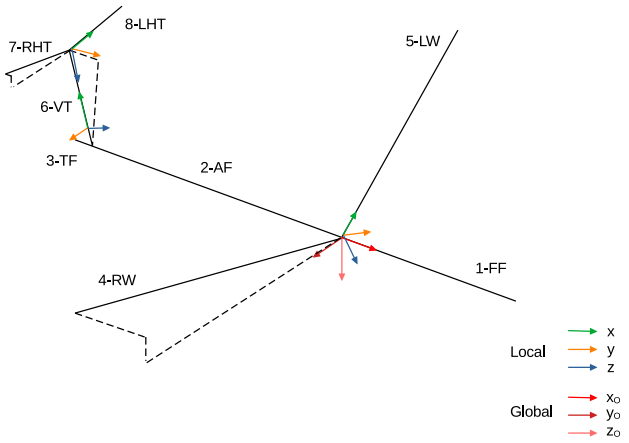

Figure 1: Aircraft discretized model.

The global coordinate system $x_0y_0z_0$ is considered coincident with the fore fuselage (FF) local coordinates. The x_0 axis points to the aircraft's nose, the y_0 axis to the right wing and the z_0 axis downward, in accordance with the right-hand rule. In Figure 1, the local coordinates of the right wing, right horizontal tail, aft and tail fuselage were omitted to have a clearer image. Table 1 describes each element, its local coordinates positions and the direction of the local x axis.

The total displacements of each component i (element) can be divided into the elastic part:

$$u_i = \sum_{r=1}^{n_x} q_r^u g_r^u(\xi) = [N^u]_i \{q_u\}_i \qquad ; \qquad v_i = \sum_{r=1}^{n_y} q_r^v f_r^v(\xi) = [N^v]_i \{q_v\}_i \tag{3}$$

$$w_i = \sum_{r=1}^{n_z} q_r^w f_r^w(\xi) = [N^w]_i \{q_w\}_i \qquad ; \qquad \phi_i = \sum_{r=1}^{n_r} q_r^\phi g_r^\phi(\xi) = \left[N^\phi\right]_i \{q_\phi\}_i \tag{4}$$

Table 1: Elements description and its local coordinates position.

Num.	Description	Abbrev.	Local coordinates origin location	x points toward
0	Global Coordinates	-	Wing-fuselage junction point	Aircraft nose
1	Fore Fuselage	FF	Wing-fuselage junction point	Aircraft nose
2	Aft Fuselage	AF	Vertical tail-fuselage junction point	Aircraft nose
3	Tail Fuselage	TF	Free tail fuselage tip	Aircraft nose
4	Right Wing	RW	Wing-fuselage junction point	Wing tip
5	Left Wing	LW	Wing-fuselage junction point	Wing tip
6	Vertical Tail	VT	Vertical tail-fuselage junction point	Vertical-horizontal tails junction point
7	Right Horizontal Tail	RHT	Vertical-horizontal tails junction point	Horizontal tail tip
8	Left Horizontal Tail	LHT	Vertical-horizontal tails junction point	Horizontal tail tip

where $[N^{u,v,w,\phi}]$ are row matrices of Bardell's shape functions and $\{q_{u,v,w,\phi}\}$ are column matrices of the system's degrees of freedom (coefficients). And the rigid part:

$$h_{x_i}(x) = \chi_{t_{x_i}} \quad \therefore \quad h_{x_i}(\xi) = \chi_{t_{x_i}} \quad ; \quad h_{y_i}(x) = \chi_{t_{y_i}} + x\chi_{r_{z_i}} \quad \therefore \quad h_{y_i}(\xi) = \left[\begin{array}{cc} 1 & \frac{(\xi+1)L_i}{2} \end{array}\right] \left\{\begin{array}{c} \chi_{t_{y_i}} \\ \chi_{r_{z_i}} \end{array}\right\} \tag{5}$$

$$h_{z_i}(x) = \chi_{t_{z_i}} - x\chi_{r_{y_i}} \quad \therefore \quad h_{z_i}(\xi) = \left[\begin{array}{cc} 1 & -\frac{(\xi+1)L_i}{2} \end{array}\right] \left\{\begin{array}{c} \chi_{t_{z_i}} \\ \chi_{r_{y_i}} \end{array}\right\} \quad ; \quad \varphi_{x_i}(x) = \chi_{r_{x_i}} \ \therefore \ \varphi_{x_i}(\xi) = \chi_{r_{x_i}} \tag{6}$$

Defining:

$$\left[\begin{array}{c} [t_{x_i}] \\ [t_{y_i}] \\ [t_{z_i}] \\ [r_{x_i}] \end{array}\right] = \left[\begin{array}{cccccc} 1 & 0 & 0 & 0 & 0 & 0 \\ 0 & 1 & 0 & 0 & 0 & (\xi+1)\frac{L_i}{2} \\ 0 & 0 & 1 & 0 & -(\xi+1)\frac{L_i}{2} & 0 \\ 0 & 0 & 0 & 1 & 0 & 0 \end{array}\right] \tag{7}$$

Writing the elastic and rigid displacements in matrix form:

$$\{d_{e_i}\} = \left\{\begin{array}{c} u_i \\ v_i \\ w_i \\ \phi_i \end{array}\right\} = \left[\begin{array}{cccc} [N^u]_i & [0] & [0] & [0] \\ [0] & [N^v]_i & [0] & [0] \\ [0] & [0] & [N^w]_i & [0] \\ [0] & [0] & [0] & [N^\phi]_i \end{array}\right] \left\{\begin{array}{c} \{q_u\}_i \\ \{q_v\}_i \\ \{q_w\}_i \\ \{q_\phi\}_i \end{array}\right\} \tag{8}$$

$$\{d_{r_i}\} = \left[\begin{array}{cccccc} 1 & 0 & 0 & 0 & 0 & 0 \\ 0 & 1 & 0 & 0 & 0 & (\xi+1)\frac{L_i}{2} \\ 0 & 0 & 1 & 0 & -(\xi+1)\frac{L_i}{2} & 0 \\ 0 & 0 & 0 & 1 & 0 & 0 \end{array}\right] \left\{\begin{array}{c} \chi_{t_{x_i}} \\ \chi_{t_{y_i}} \\ \chi_{t_{z_i}} \\ \chi_{r_{x_i}} \\ \chi_{r_{y_i}} \\ \chi_{r_{z_i}} \end{array}\right\} \quad ; \quad \{\chi_i\} = \left\{\begin{array}{c} \chi_{t_{x_i}} \\ \chi_{t_{y_i}} \\ \chi_{t_{z_i}} \\ \chi_{r_{x_i}} \\ \chi_{r_{y_i}} \\ \chi_{r_{z_i}} \end{array}\right\} \tag{9}$$

One can finally combine them as follows:

$$\{d_i\} = \{d_{e_i}\} + \{d_{r_i}\} = \underbrace{\left[\begin{array}{ccccc} [N^u]_i & [0] & [0] & [0] & [t_{x_i}] \\ [0] & [N^v]_i & [0] & [0] & [t_{y_i}] \\ [0] & [0] & [N^w]_i & [0] & [t_{z_i}] \\ [0] & [0] & [0] & [N^\phi]_i & [r_{x_i}] \end{array}\right]}_{[\mathcal{N}_i]} \underbrace{\left\{\begin{array}{c} \{q_u\}_i \\ \{q_v\}_i \\ \{q_w\}_i \\ \{q_\phi\}_i \\ \{\chi_i\} \end{array}\right\}}_{\{Q_i\}} \quad \therefore \quad \{d_i\} = [\mathcal{N}_i]\{Q_i\} \tag{10}$$

to obtain the total displacement of an arbitrary point in element i.

3.2 Structural Model of Flexible Aircraft

For the formulation of the structural model of flexible aircraft, it was first considered the Extended Hamilton's Principle, which is:

$$\delta \int_{t_1}^{t_2} \mathcal{L} dt + \delta \int_{t_1}^{t_2} W_{NC} dt = 0 \quad ; \quad \mathcal{L} = T - U \tag{11}$$

The kinetic energy T_i for the i^{th} element and its variation is:

$$T_i = \frac{1}{2}\int_{-1}^{1} \{\dot{d}_i\}^T [\mathcal{M}_i] \{\dot{d}_i\} \frac{dx}{d\xi} d\xi \qquad \therefore \qquad \delta T_i = \int_{-1}^{1} \delta\{\dot{d}_i\}^T [\mathcal{M}_i] \{\dot{d}_i\} \frac{dx}{d\xi} d\xi \tag{12}$$

where:

$$[\mathcal{M}_i] = \text{diag}(\rho_i A_i, \rho_i A_i, \rho_i A_i, I_{m_i}) \tag{13}$$

and ρ is the mass density of the material, A the cross-section area and I_m the mass moment of inertia about the beam axis. Applying the time integral:

$$\int_{t_1}^{t_2} \delta T_i dt = \int_{t_1}^{t_2}\int_{-1}^{1} \delta\{\dot{d}_i\}^T [\mathcal{M}_i] \{\dot{d}_i\} \frac{dx}{d\xi} d\xi dt = \underbrace{\int_{-1}^{1} \delta\{d_i\}^T [\mathcal{M}_i] \{\dot{d}_i\} \frac{dx}{d\xi} d\xi \Big|_{t_1}^{t_2}}_{=0} - \int_{t_1}^{t_2}\int_{-1}^{1} \delta\{d_i\}^T [\mathcal{M}_i] \{\ddot{d}_i\} \frac{dx}{d\xi} d\xi dt \tag{14}$$

where $[d_i]$ is prescribed when $t = t_1, t_2$, therefore its variation $\delta[d_i] = [0]$ on these time instances. That is the reason why the first term of the right-hand side of Equation (14) equals zero. Thus:

$$\int_{t_1}^{t_2} \delta T_i dt = \delta\{\mathcal{Q}_i\}^T \left(-\int_{t_1}^{t_2}\int_{-1}^{1} [\mathcal{N}_i]^T [\mathcal{M}_i] [\mathcal{N}_i] \{\ddot{\mathcal{Q}}_i\} \frac{dx}{d\xi} d\xi dt \right) \tag{15}$$

The total potential energy of the i^{th} element and its variation is:

$$U_i = \frac{1}{2}\int_{-1}^{1} [\varepsilon_i]^T [\mathcal{G}_i] [\varepsilon_i] \frac{dx}{d\xi} d\xi \qquad \therefore \qquad \delta U_i = \int_{-1}^{1} \delta[\varepsilon_i]^T [\mathcal{G}_i] [\varepsilon_i] \frac{dx}{d\xi} d\xi \tag{16}$$

where:

$$[\mathcal{G}_i] = \text{diag}(E_i A_i, E_i I_{zz_i}, E_i I_{yy_i}, G_i J_i) \tag{17}$$

$$[\varepsilon_i] = \underbrace{\left[\text{diag}\left(\frac{d\xi}{dx} \left[N^u_{,\xi}\right]_i, \frac{d^2\xi}{dx^2} \left[N^v_{,\xi\xi}\right]_i, \frac{d^2\xi}{dx^2} \left[N^w_{,\xi\xi}\right]_i, \frac{d\xi}{dx} [N^\phi_{,\xi}]_i \right) \quad [0] \right]}_{[N^\varepsilon]_i} \{\mathcal{Q}_i\} \tag{18}$$

and E is the modulus of elasticity, I_{zz} is the area moment of inertia with respect to the z axis, I_{yy} is the area moment of inertia with respect to the y axis, G is the shear modulus and J is the torsional constant. Therefore:

$$\delta U_i = \delta\{\mathcal{Q}_i\}^T \left(\int_{-1}^{1} {[N^\varepsilon]_i}^T [\mathcal{G}_i] [N^\varepsilon]_i \{\mathcal{Q}_i\} \frac{dx}{d\xi} d\xi \right) \tag{19}$$

For the total energy of non-conservative forces, let $\{\mathcal{F}\}$ be the column matrix of distributed loads and $\{\mathcal{P}\}$ be the column matrix of concentrated loads applied on points of coordinates $\{a\}$. Thus:

$$\delta W_{NC_i} = \delta W_{D_i} + \int_{-1}^{1} \delta\{d_i\}^T \{\mathcal{F}_i\} \frac{dx}{d\xi} d\xi + \delta\{d_i\}^T \{\mathcal{P}_i\}\Big|_{\xi=\{a\}} \tag{20}$$

where δW_{D_i} is the virtual work of viscous damping forces, defined as (Bismarck-Nasr, 1999):

$$\{f_{D_i}\} = \left[\frac{\partial \{f_{D_i}\}}{\partial \{\dot{\mathcal{Q}}_i\}} \right] \{\dot{\mathcal{Q}}_i\} = [d_{D_i}] [N^\varepsilon]_i \{\dot{\mathcal{Q}}_i\} \tag{21}$$

where $[d_{D_i}]$ is the square matrix of the damping coefficients of element i. Continuing:

$$\delta W_{D_i} = -\int_V \{f_{D_i}\}^T \delta[\varepsilon_i]\, dV = -\{\dot{\mathcal{Q}}_i\}^T \int_V \left[\frac{\partial\{f_{D_i}\}}{\partial\{\dot{\mathcal{Q}}_i\}}\right]^T \delta[\varepsilon_i]\, dV$$
$$= -\{\dot{\mathcal{Q}}_i\}^T \int_V \left[\frac{\partial\{f_{D_i}\}}{\partial\{\dot{\mathcal{Q}}_i\}}\right]^T \frac{\partial[\varepsilon_i]}{\partial\{\mathcal{Q}_i\}} dV \delta\{\mathcal{Q}_i\} = -\{\dot{\mathcal{Q}}_i\}^T \int_V [N^\varepsilon]_i^T [d_{D_i}]^T [N^\varepsilon]_i\, dV \delta\{\mathcal{Q}_i\}$$
$$= -\delta\{\mathcal{Q}_i\}^T \int_V [N^\varepsilon]_i^T [d_{D_i}] [N^\varepsilon]_i\, dV \{\dot{\mathcal{Q}}_i\} = -\int_{-1}^{1} \delta\{\mathcal{Q}_i\}^T [N^\varepsilon]_i^T [d_{D_i}] [N^\varepsilon]_i \frac{dx}{d\xi} d\xi \{\dot{\mathcal{Q}}_i\} \quad (22)$$

therefore:

$$\delta W_{NC_i} = \delta\{\mathcal{Q}_i\}^T \left(-\int_{-1}^{1} [N^\varepsilon]_i^T [d_{D_i}] [N^\varepsilon]_i \frac{dx}{d\xi} d\xi \{\dot{\mathcal{Q}}_i\} + \int_{-1}^{1} [\mathcal{N}_i]^T \{\mathcal{F}_i\} \frac{dx}{d\xi} d\xi + [\mathcal{N}_i]^T \{\mathcal{P}_i\}\Big|_{\xi=\{a\}} \right) \quad (23)$$

Substituting Equations (15), (19) and (23) into (11) and rearranging, results in:

$$\int_{t_1}^{t_2} \left\{ -\delta\{\mathcal{Q}_i\}^T \left(\int_{-1}^{1} [\mathcal{N}_i]^T [\mathcal{M}_i] [\mathcal{N}_i] \{\ddot{\mathcal{Q}}_i\} \frac{dx}{d\xi} d\xi + \int_{-1}^{1} [N^\varepsilon]_i^T [d_{D_i}] [N^\varepsilon]_i \frac{dx}{d\xi} d\xi \{\dot{\mathcal{Q}}_i\} \right.\right.$$
$$\left.\left. + \int_{-1}^{1} [N^\varepsilon]_i^T [\mathcal{G}_i] [N^\varepsilon]_i \{\mathcal{Q}_i\} \frac{dx}{d\xi} d\xi - \int_{-1}^{1} [\mathcal{N}_i]^T \{\mathcal{F}_i\} \frac{dx}{d\xi} d\xi - [\mathcal{N}_i]^T \{\mathcal{P}_i\}\Big|_{\xi=\{a\}} \right) \right\} dt = 0 \quad (24)$$

therefore:

$$\int_{-1}^{1} [\mathcal{N}_i]^T [\mathcal{M}_i] [\mathcal{N}_i] \frac{dx}{d\xi} d\xi \{\ddot{\mathcal{Q}}_i\} + \int_{-1}^{1} [N^\varepsilon]_i^T [d_{D_i}] [N^\varepsilon]_i \frac{dx}{d\xi} d\xi \{\dot{\mathcal{Q}}_i\}$$
$$+ \int_{-1}^{1} [N^\varepsilon]_i^T [\mathcal{G}_i] [N^\varepsilon]_i \frac{dx}{d\xi} d\xi \{\mathcal{Q}_i\} = \int_{-1}^{1} [\mathcal{N}_i]^T \{\mathcal{F}_i\} \frac{dx}{d\xi} d\xi + [\mathcal{N}_i]^T \{\mathcal{P}_i\}\Big|_{\xi=\{a\}} \quad (25)$$

Defining:

$$[M_i] = \int_{-1}^{1} [\mathcal{N}_i]^T [\mathcal{M}_i] [\mathcal{N}_i] \frac{dx}{d\xi} d\xi \quad ; \quad [D_i] = \int_{-1}^{1} [N^\varepsilon]_i^T [d_{D_i}] [N^\varepsilon]_i \frac{dx}{d\xi} d\xi \quad (26)$$

$$[K_i] = \int_{-1}^{1} [N^\varepsilon]_i^T [\mathcal{G}_i] [N^\varepsilon]_i \frac{dx}{d\xi} d\xi \quad ; \quad \{F_i\} = \int_{-1}^{1} [\mathcal{N}_i]^T \{\mathcal{F}_i\} \frac{dx}{d\xi} d\xi + [\mathcal{N}_i]^T \{\mathcal{P}_i\}\Big|_{\xi=\{a\}} \quad (27)$$

where $[M_i]$ is the mass matrix, $[D_i]$ is the damping matrix, $[K_i]$ is the stiffness matrix and $\{F_i\}$ is the column matrix of external loads of the i^{th} element. It finally results in:

$$[M_i]\{\ddot{\mathcal{Q}}_i\} + [D_i]\{\dot{\mathcal{Q}}_i\} + [K_i]\{\mathcal{Q}_i\} = \{F_i\} \quad (28)$$

In order to assure the connection between elements, it is necessary to define the continuity equations. They are described in terms of the 3 degrees of freedom of translation and the 3 degrees of freedom of rotation. Let the following equations be those that define the continuity of the element i on point $\xi = a_1$ and the element j on point $\xi = a_2$:

$$\left[C_{i/0}\right]^T \left[d^i_{xyz}\right]\Big|_{\xi=a_1} = \left[C_{j/0}\right]^T \left[d^j_{xyz}\right]\Big|_{\xi=a_2} \quad ; \quad \left[C_{i/0}\right]^T \left[d^i_{rots}\right]\Big|_{\xi=a_1} = \left[C_{j/0}\right]^T \left[d^j_{rots}\right]\Big|_{\xi=a_2} \quad (29)$$

where:

$$[d_{xyz}] = \begin{bmatrix} [N^u] & [0] & [0] & [0] & [t_x] \\ [0] & [N^v] & [0] & [0] & [t_y] \\ [0] & [0] & [N^w] & [0] & [t_z] \end{bmatrix} \{\mathcal{Q}\} = [N_{xyz}]\{\mathcal{Q}\} \quad (30)$$

$$[d_{rots}] = \begin{bmatrix} [0] & [0] & [0] & [N^\phi] & [r_x] \\ [0] & [0] & -\left[N^w_{,\xi}\right]\frac{d\xi}{dx} & [0] & -[t_{z,\xi}]\frac{d\xi}{dx} \\ [0] & \left[N^v_{,\xi}\right]\frac{d\xi}{dx} & [0] & [0] & [t_{y,\xi}]\frac{d\xi}{dx} \end{bmatrix} \{\mathcal{Q}\} = [N_{rots}]\{\mathcal{Q}\} \quad (31)$$

and $[C_{i/0}]$ is the transformation matrix from global to local coordinates and has the property that $[C_{i/0}]^T = [C_{0/i}]$. With those continuity equations, it is possible to build the condensation matrix $[T]$, which, as the name suggests, condensates the matrices, eliminating the doubled degrees of freedom that are equal. This process is described by Guimarães Neto (2020) and hereafter by Guimarães Neto (2021).

Now, concerning the whole aircraft, its matrices are defined as:

$$[M_{total}] = \text{diag}\left([M_1], [M_2], \cdots, [M_{n_{elem}}]\right) \quad ; \quad [D_{total}] = \text{diag}\left([D_1], [D_2], \cdots, [D_{n_{elem}}]\right) \tag{32}$$

$$[K_{total}] = \text{diag}\left([K_1], [K_2], \cdots, [K_{n_{elem}}]\right) \quad ; \quad \{F_{total}\} = \begin{Bmatrix} \{F_1\} \\ \{F_2\} \\ \vdots \\ \{F_{n_{elem}}\} \end{Bmatrix} \tag{33}$$

where n_{elem} is the total number of elements in the structural model. Then, condensing the matrices:

$$\left[\overline{M}\right] = [T]^T [M_{total}] [T] \; ; \; \left[\overline{D}\right] = [T]^T [D_{total}] [T] \; ; \; \left[\overline{K}\right] = [T]^T [K_{total}] [T] \; ; \; \left\{\overline{F}\right\} = [T]^T \{F_{total}\} \tag{34}$$

For a dynamic analysis, it leads to:

$$[\overline{M}]\{\ddot{\overline{\mathcal{Q}}}\} + [\overline{D}]\{\dot{\overline{\mathcal{Q}}}\} + [\overline{K}]\{\overline{\mathcal{Q}}\} = \{\overline{F}\} \tag{35}$$

then, for an undamped free vibration analysis:

$$[\overline{M}]\{\ddot{\overline{\mathcal{Q}}}\} + [\overline{K}]\{\overline{\mathcal{Q}}\} = \{0\} \qquad \therefore \qquad \left(\left[\overline{K}\right] - \lambda \left[\overline{M}\right]\right) \left\{\overline{\Delta}\right\} = \{0\} \tag{36}$$

where $\lambda = (2\pi f)^2$ is an eigenvalue and $\{\overline{\Delta}\}$ is an eigenvector. Therefore:

$$f = \frac{\sqrt{\lambda}}{2\pi} \quad \text{[Hz]} \quad ; \quad \{\Delta\} = [T] \left\{\overline{\Delta}\right\} \tag{37}$$

3.2.1 Inclusion of Effects of Concentrated Masses

Let a concentrated mass be considered, for which $\vec{r}_m$ is the position vector of the point mass with respect to the point it is attached on the element, $\vec{V}_b$ is the beam velocity vector at that point, $\vec{\omega}_{m/b}$ is the angular velocity vector of the point mass relative to the beam, $[J_m]$ is the inertia matrix of the concentrated mass and m_m is its mass. Therefore, the kinetic energy of this point mass is defined as:

$$T_m = \frac{1}{2} m_m \{V_b\}^T \{V_b\} - m_m \{V_b\}^T [\widetilde{r_m}] \{\omega_{m/b}\} + \frac{1}{2} \{\omega_{m/b}\}^T \left(m_m [\widetilde{r_m}]^T [\widetilde{r_m}] + [J_m]\right) \{\omega_{m/b}\} \tag{38}$$

Defining:

$$\{V_b\} = [\dot{d}_{xyz}] = [N_{xyz}]\{\dot{\mathcal{Q}}\} \quad ; \quad \{\omega_{m/b}\} = [\dot{d}_{rots}] = [N_{rots}] \{\dot{\mathcal{Q}}\} \tag{39}$$

therefore:

$$T_m = \frac{1}{2} m_m \{\dot{\mathcal{Q}}\}^T [N_{xyz}]^T [N_{xyz}] \{\dot{\mathcal{Q}}\} - m_m \{\dot{\mathcal{Q}}\}^T [N_{xyz}]^T [\widetilde{r_m}] [N_{rots}] \{\dot{\mathcal{Q}}\} + \frac{1}{2} \{\dot{\mathcal{Q}}\}^T [N_{rots}]^T \left(m_m [\widetilde{r_m}]^T [\widetilde{r_m}] + [J_m]\right) [N_{rots}] \{\dot{\mathcal{Q}}\} \tag{40}$$

The procedure of the derivation for the mass matrix is the same of the beam element. Therefore, the mass matrix of a concentrated mass attached to a point $\xi = a$ in an arbitrary beam element is defined as the following:

$$[M_m] = \Big(m_m [N_{xyz}]^T [N_{xyz}] - m_m [N_{xyz}]^T [\widetilde{r_m}] [N_{rots}] + m_m [N_{rots}]^T [\widetilde{r_m}] [N_{xyz}] + [N_{rots}]^T \left(m_m [\widetilde{r_m}]^T [\widetilde{r_m}] + [J_m]\right) [N_{rots}] \Big)\Big|_{\xi=a} \tag{41}$$

consequently, the total mass matrix of an element i, considering a total of n masses attached to it, is:

$$[M_{i+m}] = [M_i] + \sum_{j=1}^{n} \left[M_{m_j}\right] \tag{42}$$

It is important to clarify how the distance vector $\vec{r}_m$ for each mass element m_m was defined. For every mass element, it was attempted to define a distance vector perpendicular to the beam element axis. Sometimes it was not possible to have a perpendicular vector, due to its local x coordinate be out of the beam element domain. In these cases, the distance vector was calculated using the last valid local x coordinate, regardless of the angle between the vector and the beam element axis.

4. RESULTS

It was created an example structure of an aircraft in FEMAP®, using classical finite elements in order to verify the HFEM formulation of Section 3, which was implemented in MATLAB®. It was considered a typical aluminum alloy for all components of the aircraft, with the following characteristics: elasticity modulus $E = 73.1$ GPa, Poisson's ratio $\nu = 0.33$ and mass density $\rho = 2780$ kg/m^3.

The geometry of each element of the aircraft is described in Table 2, where area, moments of inertia and torsional constant are in relation to the cross-section:

Table 2: Geometry of each element of the aircraft.

Nº	Length [m]	Area [m²]	I_{yy} [m^4]	I_{zz} [m^4]	J [m^4]
1	7.5	0.785	0.049	0.049	0.098
2	7	0.785	0.049	0.049	0.098
3	1	0.785	0.049	0.049	0.098
4	8.5	0.125	$6.510 \cdot 10^{-4}$	0.003	0.002
5	8.5	0.125	$6.510 \cdot 10^{-4}$	0.003	0.002
6	3	0.02	$6.667 \cdot 10^{-5}$	$1.667 \cdot 10^{-5}$	$4.579 \cdot 10^{-5}$
7	3	0.008	$4.267 \cdot 10^{-6}$	$6.667 \cdot 10^{-6}$	$8.802 \cdot 10^{-6}$
8	3	0.008	$4.267 \cdot 10^{-6}$	$6.667 \cdot 10^{-6}$	$8.802 \cdot 10^{-6}$

The main purpose was to compare the natural frequencies and mode shapes as well as to verify the mathematics and algorithm to build the mass and stiffness matrices as well as the condensation matrix.

A simple convergence procedure was performed for both classical and hierarchical FEM models. For the classical FEM, the mesh refinement was performed once, increasing the number of elements by 5 times in one step. With this refinement procedure, the resultant values of the mode frequencies did not change. Regarding the hierarchical FEM, the convergence analysis was performed by increasing the number of equations for each structural degree of freedom of each element, starting with 4, ceasing when the values of the mode frequencies did not significantly change and were close to those of the classical FEM. The classical FEM model was made with 415 beam elements whereas, in the HFEM, 10 equations (including the boundary condition functions) from Bardell's series were used for each degree of freedom of each element, which results in 320 equations to solve. All elements had cantilever boundary conditions: elements 1, 4-8 were fixed at $\xi = -1$ and free at $\xi = 1$ and elements 2 and 3 the other way, free at $\xi = -1$ and fixed at $\xi = 1$.

While in the classical FEM there is more flexibility regarding the method of how to implement the boundary conditions and how to attach the concentrated masses (on nodes, specific element position, points, lines, etc), the hierarchical FEM does not offer such flexibility, since nodes are not used in the elements domain. The boundary conditions must be implemented by means of geometric position as well as the concentrated masses.

With the characteristics, parameters and boundary conditions previously mentioned, it was possible to run the implementation and compare the modal analysis results. Figure 2 shows this comparison.

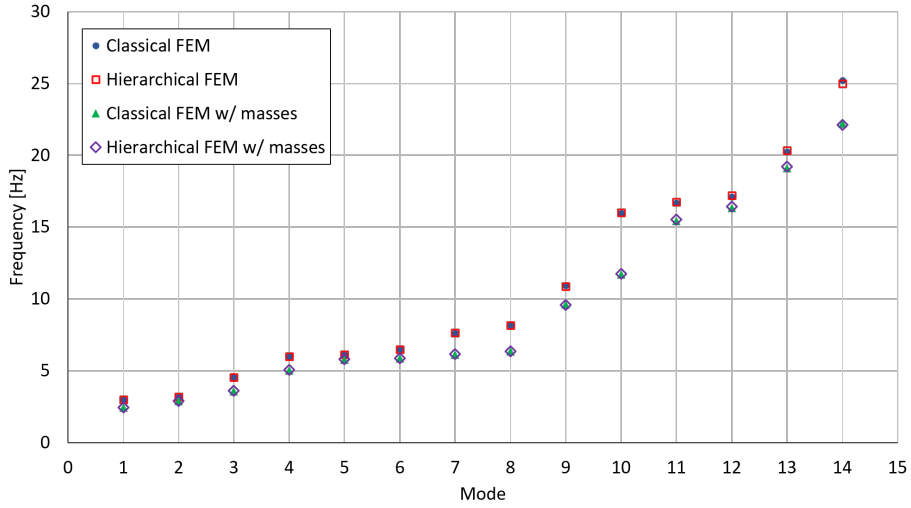

Figure 2: Comparison of results for modal frequencies.

In Figure 2, it is possible to notice the accuracy of the Bardell's series, with a maximum deviation of 0.9% in the frequency of the last mode.

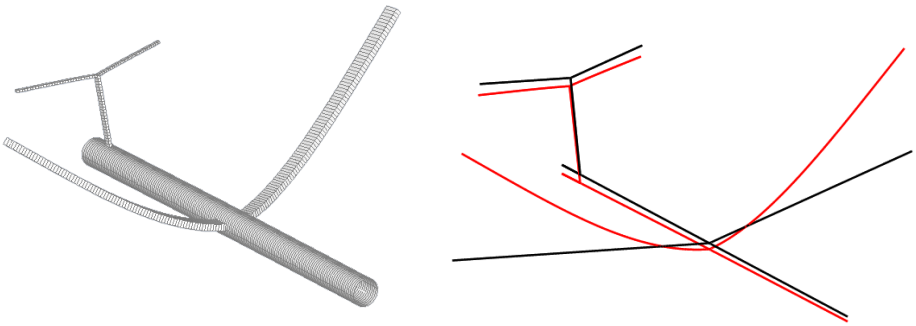

(a) Classical FEM (b) Hierarchical FEM

Figure 3: 1st vibration mode.

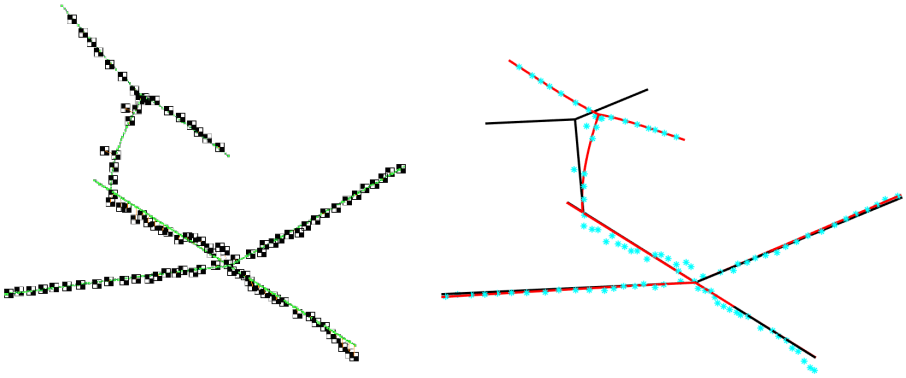

(a) Classical FEM (b) Hierarchical FEM

Figure 4: 1st vibration mode (with concentrated masses).

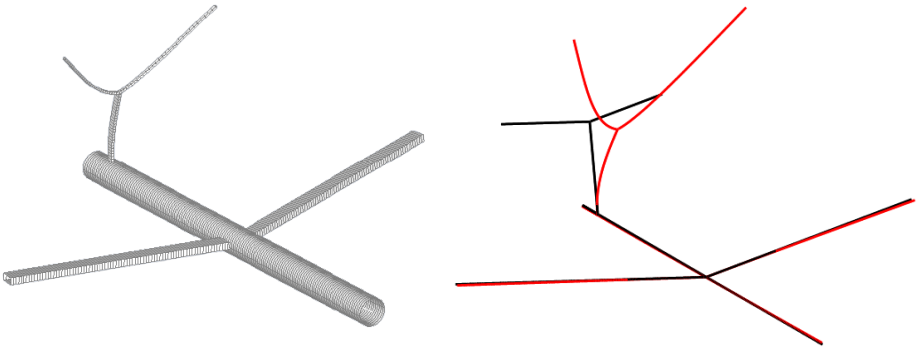

(a) Classical FEM (b) Hierarchical FEM

Figure 5: 6th vibration mode.

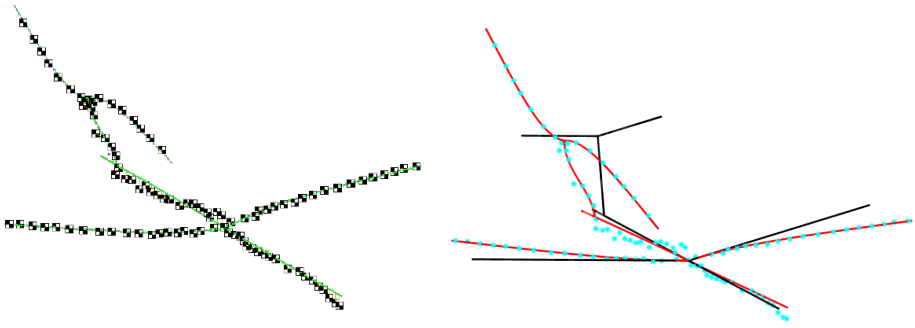

(a) Classical FEM (b) Hierarchical FEM

Figure 6: 6th vibration mode (with concentrated masses).

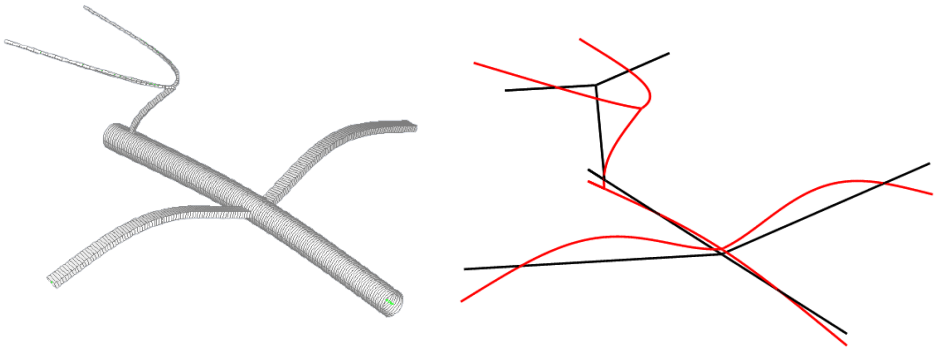

(a) Classical FEM (b) Hierarchical FEM

Figure 7: 11$^{\text{th}}$ vibration mode.

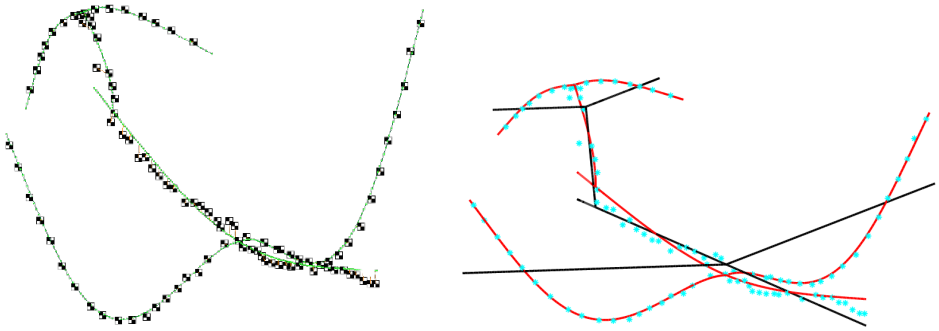

(a) Classical FEM (b) Hierarchical FEM

Figure 8: 11$^{\text{th}}$ vibration mode (with concentrated masses).

Figures 3, 5 and 7 exhibit 3 vibration modes of the aircraft: 1 low, 1 medium and 1 high frequency modes. Good agreement is observed for all the mode shapes.

For the analysis with the concentrated masses, the data for these masses can be found in the appendix section of the NASA report (Meirovitch and Tuzcu, 2003). The same characteristics, parameters and boundary conditions of the previous comparison were used. The results are shown in Figure 2 as well.

Again, the accuracy of the Bardell's series is remarkable, with a maximum deviation in frequencies of 0.77%. Figures 4, 6 and 8 expose the mode shapes of a low, a medium, and a high frequency mode.

5. CONCLUSIONS

The Bardell's hierarchical equations were shown to be suitable for modeling aircraft structures. They have very satisfactory accuracy when compared with classical FEM, are simple to implement and favor a quick, easy and seamless possibility of change of the aircraft geometry and structural properties.

The hierarchical formulation of the finite element has excellent results when both the modal frequencies and mode shapes are compared with the classical formulation. It has the potential to reduce computational cost for calculating the structural dynamics of flexible aircraft, when the possibility of previously gathering and storing a high quantity of Bardell's shape functions and pre-calculated matrices – mass and stiffness, for instance – is considered. It is also noticeable the possibility of easily changing simple geometric properties, such as the dihedral and sweep angles of the wing or the horizontal empennage in the hierarchical finite element model. This is certainly an advantage in early phases of aircraft design.

This new modeling paradigm of the aircraft structure can also help in optimization processes with its great potential of reducing required computer resources when compared with classical FEM. Furthermore, it has the potential of increasing the speed and allowing automatic convergence analysis as well as parameterization of input data, such as geometry and material properties.

6. REFERENCES

Babuška, I., 1988. "The p and h-p versions of the finite element method". In D.L. Dwoyer, M.Y. Hussaini and R.G. Voigt, eds., *Finite Elements*. Springer, New York, NY, pp. 199–239.

Babuška, I., Szabo, B.A. and Katz, I.N., 1981. "The p-version of the finite element method". *Journal on Numerical Analysis*, Vol. 18, No. 3, pp. 515–545.

Bardell, N.S., 1989. "The application of symbolic computing to the hierarchical finite element method". *International Journal for Numerical Methods in Engineering*, Vol. 28, No. 5, pp. 1181–1204. ISSN 0029-5981. doi: 10.1002/nme.1620280513.

Bardell, N.S., 1991. "Free vibration analysis of a flat plate using the hierarchical finite element method". *Journal of Sound and Vibration*, Vol. 151, No. 2, pp. 263–289. ISSN 10958568. doi:10.1016/0022-460X(91)90855-E.

Bernardino, B.N.S., 2019. *Análise de Estabilidade em Painéis Planos Enrijecidos Trincados pelo Método de Rayleigh-Ritz*. Master's thesis, Graduate Program of Aeronautical and Mechanical Engineering, Instituto Tencnológia de Aeronáutica, São José dos Campos, Brazil.

Beslin, O. and Nicolas, J., 1997. "A hierarchical functions set for predicting very high order plate bending modes with any boundary conditions". *Journal of Sound and Vibration*, Vol. 202, No. 5, pp. 633–655. ISSN 0022460X. doi: 10.1006/jsvi.1996.0797.

Bismarck-Nasr, M.N., 1999. *Structural Dynamics in Aeronautical Engineering*. AIAA education series. Reston, VA.

De-Chao, Z., 1986. "Development of Hierarchal Finite Element Methods at BIAA". In G. Yagawa and S. Atluri, eds., *Computational Mechanics '86*. Springer, Tokyo, pp. 159–164.

de Sena e Oliveira, B.H., 2018. *Uso do Método de Ritz na Análise de Placas Reforçadas na Presença de Trincas*. Master's thesis, Graduate Program of Aeronautical and Mechanical Engineering, Instituto Tencnológia de Aeronáutica, São José dos Campos, Brazil.

Guimarães Neto, A.B., 2020. "Modeling and simulation of flexible aircraft". 14 chapters. Class notes of subject AB-276.

Guimarães Neto, A.B., 2021. "Modeling of unrestrained flexible aircraft structures based on the Rayleigh-Ritz method". Submitted to the AIAA Journal.

Meirovitch, L. and Tuzcu, I., 2003. "Integrated approach to the dynamics and control of maneuvering flexible aircraft". Technical report, NASA, Hampton. URL `https://ntrs.nasa.gov/search.jsp?R=20030062109`. NASA/CR-2003-211748 Report.

Zienkiewicz, O.C., de S. R. Gago, J.P. and Kelly, D.W., 1983. "The hierarchical concept of finite element analysis". *Computers and Structures*, Vol. 16, No. 1–4, pp. 53–65.

7. RESPONSIBILITY NOTICE

The authors are solely responsible for the printed material included in this paper.